

---

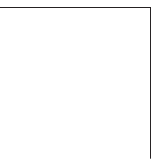
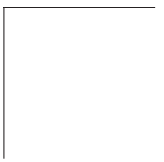
# Contents

---

<b>Contents</b>	<b>i</b>
<b>List of Figures</b>	<b>v</b>
<b>List of Tables</b>	<b>x</b>
<b>1 Introduction</b>	<b>1</b>
1.1 General context . . . . .	1
1.2 Objectives and methodology . . . . .	4
1.3 Thesis outline . . . . .	7
References . . . . .	8
<b>2 Urea water injection process</b>	<b>13</b>
2.1 Introduction . . . . .	13
2.2 Emissions and pollutants from internal combustion engines . . . . .	13
2.2.1 European regulations on automotive internal combustion engines pollutant emissions . . . . .	14
2.2.2 The homologation cycles . . . . .	15
2.2.3 NO <sub>x</sub> formation process in Internal Combustion Engines	19
2.2.4 NO <sub>x</sub> formation process in Compression Ignition Engines	22
2.2.5 NO <sub>x</sub> Reduction strategies for diesel engines . . . . .	24
2.3 Selective catalytic reduction systems . . . . .	28
2.3.1 SCR operating principle . . . . .	30
2.3.2 Components of a SCR system . . . . .	33
2.3.3 UWS dosing unit . . . . .	35
2.3.4 Hydraulic characterization of UWS injector . . . . .	38
2.3.5 Spray development characterization of UWS injectors . .	39

2.4 Spray atomization process . . . . .	45
2.4.1 Secondary atomization . . . . .	48
2.5 Summary . . . . .	50
References . . . . .	51
<b>3 Materials and Methods</b>	<b>57</b>
3.1 Introduction . . . . .	57
3.2 Injection system . . . . .	57
3.2.1 Dosing system in the laboratory . . . . .	58
3.3 Momentum flux . . . . .	63
3.3.1 Measurement setup . . . . .	66
3.3.2 Measurement procedure . . . . .	66
3.4 Injected mass . . . . .	67
3.4.1 Measurement setup . . . . .	67
3.4.2 Measurement procedure . . . . .	68
3.5 Rate of injection . . . . .	68
3.6 High flow and high temperature installation for UWS spray visualization . . . . .	71
3.6.1 Hot-air flow test rig . . . . .	72
3.6.2 Control elements and sensors . . . . .	73
3.7 Optical techniques . . . . .	79
3.7.1 Diffused back-illumination . . . . .	79
3.8 Image processing methods . . . . .	80
3.8.1 Spray penetration and spreading angle . . . . .	80
3.9 Summary . . . . .	86
References . . . . .	87
<b>4 UWS Hydraulic performance</b>	<b>91</b>
4.1 Introduction . . . . .	91
4.2 Hydraulic characterization test plan . . . . .	91
4.3 Momentum flux results . . . . .	92
4.4 Injected mass results . . . . .	99
4.5 Rate of injection results . . . . .	100
4.6 Discharge Coefficient . . . . .	102
4.7 Summary and conclusions . . . . .	105
References . . . . .	106
<b>5 Spray penetration and spreading angle of UWS injection systems</b>	<b>109</b>
5.1 Introduction . . . . .	109

5.2	Spray characterization test plan . . . . .	109
5.3	Spray penetration . . . . .	110
5.3.1	Spray Segmentation of burst and spray body . . . . .	111
5.3.2	Spray penetration behaviour at 90 degree position. . . . .	115
5.3.3	Spray penetration behaviour at 45 degree position. . . . .	118
5.4	Spray spreading angle . . . . .	121
5.5	Summary and conclusions . . . . .	124
	References . . . . .	126
<b>6</b>	<b>Droplet Characterization</b>	<b>129</b>
6.1	Introduction . . . . .	129
6.2	Test plan . . . . .	129
6.3	Droplet size distribution . . . . .	132
6.3.1	Droplet size determination . . . . .	132
6.3.2	Effect of injection pressure on the droplet size distribution	136
6.4	Droplet velocity distribution . . . . .	139
6.5	Velocity determination and validation of the measurement technique . . . . .	140
6.5.1	Effect of injection pressure on droplet velocity . . . . .	142
6.5.2	Effect of the flow temperature on droplet velocity . . . . .	145
6.5.3	Droplet diameter - velocity relationship . . . . .	146
6.5.4	Dimensionless numbers and atomization regimes . . . . .	147
6.6	Summary and conclusions . . . . .	152
	References . . . . .	153
<b>7</b>	<b>Conclusions and future works</b>	<b>157</b>
7.1	Summary . . . . .	157
7.2	Future Works . . . . .	162
	<b>Global Bibliography</b>	<b>165</b>



---

# List of Figures

---

2.1	EURO Standards maximum limits for PM and NO <sub>x</sub> in light duty diesel engines [2]. . . . .	16
2.2	New European Driving Cycle (NEDC) velocity profile over time (Adapted from [3]). . . . .	17
2.3	Worldwide harmonized Light duty vehicles Test Cycle (WLTC) velocity profile curve over time(Adapted from [3]). . . . .	18
2.4	Relative concentrations for the three different formation of nitrogen oxides (thermal, prompt, fuel), with the increase of flame temperature [6]. . . . .	20
2.5	Particulate matter vs NO <sub>x</sub> trade-off [9]. . . . .	24
2.6	Methods to reduce pollutant emissions for Diesel engines [8]. . . . .	25
2.7	Example of an SCR system. . . . .	28
2.8	Freezing point of the solution versus concentration of urea. [13] . . . . .	29
2.9	Bosch Denoxtronic 1.1 system components for heavy duty vehicles (Adapted from [16]). . . . .	33
2.10	Bosch Denoxtronic 5.0 system components (Adapted from [16]). . . . .	34
2.11	Exhaust line "Y" layout. . . . .	35
2.12	Air-cooled UWS injector. . . . .	36
2.13	Liquid-cooled UWS injector. . . . .	37
2.14	Example of deposit formation in a commercial nozzle. . . . .	38
2.15	Visualization test rig and optical setup used in [29]. . . . .	40
2.16	Scheme of the flow rig and visualization chamber used in [30]. . . . .	41
2.17	Diagram of the visualization system used in [32]. . . . .	42
2.18	Test rig used in [33]. Left side: Laser backlight imaging setup. Right side: PDA arrangement. . . . .	43
2.19	Laser backlight imaging setup used in [2]. . . . .	44
2.20	Experimental setup with shadowgraphy and microscope used in [36]. . . . .	44

2.21	Break-up regimes at the tested conditions of [36], based on [38, 39].	46
2.22	Diagram of the jet breakup regimes classification (extracted from [41]).	47
2.23	Breakup regimes for a low viscosity Newtonian droplet in a horizontal air stream	49
3.1	Schematic diagram of the dosing system adapted to laboratory requirements.	58
3.2	Pressure unit schematic diagram.	59
3.3	Dosing unit.	60
3.4	Geometrical characterization of the hole outlet with the optical microscope.	61
3.5	Internal inspection of the nozzle using X-rays tomography.	62
3.6	Injector signal controller. a) Engine Control Unit from Bosch. b) Commercial injector driver.	63
3.7	Electrical signal definition.	63
3.8	Temperature controller.	64
3.9	Spray momentum flux measurement principle.	65
3.10	Diagram momentum flux test rig.	66
3.11	Injection Measurement setup schematic diagram.	68
3.12	(a) Representation of the real flow behaviour: area, density and velocity profile. (b) Representation of the effective area, density, and effective velocity in a nozzle. Adapted from [1].	69
3.13	Hot-air flow test rig.	73
3.14	Configuration of the optically-accessible section.	74
3.15	Diagram of the visualization test rig setup.	74
3.16	Test bench used for the flow meter calibration.	75
3.17	Calibration curves of the mass flow meter.	76
3.18	Mass flow meter and thermocouples used in the high flow test rig.	76
3.19	Temperature control flange.	77
3.20	Pressure gauges employed in the installation.	78
3.21	Electrical board of the installation.	78
3.22	Diagram of the diffused back-illumination setup used for the visualization of the spray.	80
3.23	Classic contour detecting algorithm (red lines) and region of droplets that are not detected (blue lines).	81
3.24	Sketch of the UWS spray morphology and burst definition	81
3.25	Binary image alongside the cumulative pixel count curve for four different time steps.	83
3.26	Measuring distances for the spray angle determination	84

---

3.27	Schematic diagram of the diffused back-illumination setup used for the visualization of the droplets. . . . .	84
3.28	Steps for the detection of the droplets at each frame:( <b>a</b> ) Image with subtracted background. ( <b>b</b> ) Binarized image. ( <b>c</b> ) Detection of the droplet. ( <b>d</b> ) Tagged droplets. . . . .	86
3.29	Trajectory of droplets at different frames: ( <b>a</b> ) 1780 $\mu$ s, ( <b>b</b> ) 1806 $\mu$ s, and ( <b>c</b> ) 1838 $\mu$ s After Start of Energizing. . . . .	87
4.1	Signal of Momentum flux at four distances between nozzle and sensor	93
4.2	Images of the spray at 4 mm from the hole exit. Time is measured After Start Of Energizing (ASOE). . . . .	94
4.3	Momentum flux signal. Injection pressure: 5 bar (absolute). Discharge pressure: 0.75 bar (absolute). Cooling temperature: 60 °C. (Time ASOE). . . . .	95
4.4	Momentum flux for water (left) and UWS (right). Influence of the injection pressure and discharge pressure. . . . .	96
4.5	Momentum flux for water (left) and UWS (right). Influence of the cooling temperature. . . . .	96
4.6	Comparison of the spray momentum flux for both fluids. . . . .	97
4.7	(left) Average momentum flux for all tested conditions. (right) Ratio of the average momentum flux between water and UWS. . . . .	98
4.8	Comparison of the injected mass. (Left) Water. (Right) UWS. . . . .	99
4.9	Rate of injection curves. Comparison of injection pressure effect at three cooling temperatures and 1 bar of discharge pressure. . . . .	101
4.10	Averaged rate of injection as a function of $\Delta P^{0.5}$ . (Left) Water. (Right) UWS. . . . .	102
4.11	Viscosity of the UWS and water at different temperatures. . . . .	103
4.12	Discharge coefficient vs Reynolds number for water (left side) and UWS (right side). . . . .	104
4.13	Section view of the internal geometry of the studied injector. . . . .	105
5.1	Injector positioning inside of the visualization chamber at 45° (left) and 90° (right) inclination angles regarding the air mass flow. . . . .	111
5.2	Spray burst and body evolution at 1.1, 1.6 and 2.2 ms measured from the start of energizing. The upper row represents the injection pressure of 4 bar and the lower 8 bar. . . . .	113
5.3	Spray burst and body comparison for all injection pressures and cooling temperature of 60°C, time after start of energizing. . . . .	114
5.4	Spray burst and body comparison for all injection pressures and cooling temperature of 90°C . . . . .	114

5.5	Spray burst and body comparison for all injection pressures and cooling temperature of 120°C . . . . .	115
5.6	Comparison of the spray Burst and Body for different air mass flows and injector cooling temperature of 60 °C . . . . .	116
5.7	Comparison of the spray Burst and Body for different air mass flows and injector cooling temperature of 90 °C . . . . .	117
5.8	Comparison of the spray Burst and Body for different air mass flows and injector cooling temperature of 120°C . . . . .	117
5.9	Spray burst and body comparison for all injection pressures and cooling temperature of 60°C . . . . .	118
5.10	Spray burst and body comparison for all injection pressures and cooling temperature of 90°C . . . . .	119
5.11	Effect of injection pressure at a UWS cooling temperature of 60°C	119
5.12	Effect of injection pressure at a UWS cooling temperature of 90°C	120
5.13	Effect of the injection pressure, air mass flow, and injector positioning on the spray spreading angle. . . . .	122
5.14	Average angles from the steady part of the spray at a cooling temperature of 60°C . . . . .	123
5.15	Average angles from the steady part of the spray at a cooling temperature of 90°C . . . . .	123
5.16	Average angles from the steady part of the spray at a cooling temperature of 120°C . . . . .	124
6.1	Location of the windows used for the near-field visualization (not to scale). P1: Position 1, P2: Position 2, P3: Position 3. . . . .	131
6.2	Images of the UWS droplets at two positions of the spray. Top row: Position P1. Bottom row: P2. For three injection pressures: 4 bar (A and D), 6 bar (B and E), and 8 bar (C and F ). Gas temperature: 180 °C. . . . .	133
6.3	Droplet diameter PDF for three different techniques at position P2. Injection pressure: 6 bar. . . . .	135
6.4	Distribution of the droplet diameter at position P1 (near the nozzle exit) for the three injection pressures. . . . .	137
6.5	Distribution of the droplet diameter at position P2, for the three injection pressures. . . . .	138
6.6	Distribution of the droplet diameter at position P3, for the three injection pressures. . . . .	139
6.7	Droplet morphology identification in position P2 ( Y = 30 mm) at different time steps. Injection pressure: 4, 6 and 8 bar. Technique: HSMI . . . . .	140

---

6.8 Sauter Mean Diameter (SMD) evolution over injection time. Injection pressure: 4, 6 and 8 bar. . . . .	141
6.9 Droplet velocity versus diameter comparison for both measuring techniques. . . . .	142
6.10 Droplet average velocity in Y direction measured by PDA and HSMV for three pressure levels. . . . .	143
6.11 Droplet velocity distribution in the Y axis at position P1, for the three injection pressures. . . . .	144
6.12 Droplet velocity distribution in the Y axis at position P2, for the three injection pressures. . . . .	145
6.13 Droplet velocity distribution in the Y axis at position P3, for the three injection pressures. . . . .	146
6.14 Distribution of the droplet velocity in the X axis at P1, for the three injection pressures. . . . .	147
6.15 Distribution of the droplet velocity in the X axis at P2, for the three injection pressures. . . . .	148
6.16 Distribution of the droplet velocity in the X axis at P3, for the three injection pressures. . . . .	149
6.17 Droplet velocity distribution in the Y axis. Position P1 (left), Position P2 (center), and Position P3 (right), Gas-flow temperatures: 180 and 350 °C. . . . .	149
6.18 Droplet velocity distribution in the X axis. Position P1 (left), Position P2 (center), and Position P3 (right), Gas-flow temperatures: 180 and 350 °C. . . . .	150
6.19 Normalized droplet and velocity relationship. . . . .	150
6.20 Primary breakup regime for the three pressure levels tested. . . . .	151
6.21 Second Atomization regime for the three pressure levels tested. . . . .	152
7.1 Urea deposits in the injector nozzle tip . . . . .	163

---

# List of Tables

---

2.1	Real Driving Emission test trip speed and distance characteristics.	19
3.1	Injector technical features. . . . .	60
3.2	Momentum Flux test rig properties. . . . .	67
4.1	Experimental conditions. . . . .	92
5.1	Test plan for the macroscopic spray visualization campaign. . . . .	110
6.1	Test plan for the droplet characterization. . . . .	130
6.2	Details of the optical setup for the DBI: Near field spray measurements. . . . .	132